Engineering Structures 85 (2015) 1–10

Contents lists available at ScienceDirect

Engineering Structures

journal homepage: www.elsevier.com/locate/engstruct

Application of Nonlinear-Autoregressive-Exogenous model to predict the hysteretic behaviour of passive control systems

Ricky W.K. Chan [a], Jason K.K. Yuen [b], Eric W.M. Lee [b,*], Mehrdad Arashpour [c]

[a] School of Civil, Environmental and Chemical Engineering, RMIT University, Melbourne, Australia
[b] Department of Civil and Architectural Engineering, City University of Hong Kong, Kowloon Tong, Hong Kong, China
[c] School of Property, Construction and Project Management, RMIT University, Melbourne, Australia

ARTICLE INFO

Article history:
Received 27 March 2014
Revised 2 December 2014
Accepted 4 December 2014
Available online 23 December 2014

Keywords:
Nonlinear autoregressive model
Hysteretic behaviour
Steel slit damper
Yielding shear panel device

ABSTRACT

This paper proposes to use the nonlinear-autogressive models with exogenous input (NARX) model to predict the hysteretic behaviour of passive control systems. Although existing analytical hysteresis models such as the generalized Bouc–Wen (BW) model and the Bouc–Wen–Baber–Noori (BWBN) model can be used to model the hysteretic behaviour of passive control systems, the generalized BW model fails to account the pinching or stiffness degradation of hysteretic systems and the BWBN model requires to tune considerable parameters before its application. Therefore, we propose this alternative approach to predict the hysteresis response of passive control systems. The NARX model is the branch of artificial intelligence which is a promising tool for the forecasting of time series problems. We adopted the NARX model to predict the hysteretic behaviour with experimental results conducted on yielding shear panel device (YSPD) and steel slit damper (SSD), respectively. A good agreement between the experimental results on both YSPD and SSD and the prediction results was achieved. We also combined the NARX model and the general regression neural network (GRNN) as a hybrid model to predict hysteretic behaviour of the SSD of which the damper design was hidden from the model training process. The performance of using the hybrid model to predict the hysteretic behaviour of SSD is reasonably well. Finally, the applicability of the hybrid model has been successfully demonstrated through the optimisation of the geometrical parameters of the SSD. We concluded that the proposed NARX model is capable to predict the hysteretic behaviour of passive control systems.

1. Introduction

The past two decades have seen the development of a number of different kinds of structural controls for minimizing the damage of the structures caused by earthquake excitation [1,2]. These structural controls can be broadly divided into passive control systems, active control systems and semi-control systems. Passive control systems, also known as passive energy dissipation systems refer to the systems which do not require any external source of power. It can be achieved by equipping the dampers or designated devices into the structures. In contrast, active control systems refer to the systems which require an external source of power to generate structural control forces. It can be achieved by equipping the real-time processing sensors with force delivery devices into the structures and semi-active control systems refer to the systems which require little power to change certain structural parameters. Unlike active control systems or the semi-active control systems, passive control systems do not require an external source of power, the reliability associated with power supply and computer control during the earthquake event is thus eliminated [3]. In addition, by strategically locating the dampers or designated devices in the structure, replacement of the damaged dampers or designated devices can be carried out. Therefore, the passive energy dissipation systems have been considered as an inexpensive and effective way to mitigate the risks caused by earthquake excitation to the structures.

A number of passive energy dissipation devices such as ADAS [4,5], SSD [3], YSPD [6], TTD [7] and hourglass-shaped copper energy dissipation devices [8] which rely on plastic behaviour of metals have been proposed. They are usually incorporated in framed structures by connecting the devices between brace systems and floor beams as shown in Fig. 1 while other devices are designed for installation between beams and columns [9]. The resulting combined lateral stiffness is equivalent to the stiffness of the device and the brace connected in series, in addition to the

* Corresponding author. Tel.: +852 3442 2307; fax: +852 3442 0427.
E-mail address: ericlee@cityu.edu.hk (E.W.M. Lee).

http://dx.doi.org/10.1016/j.engstruct.2014.12.007
0141-0296/

stiffness of the structure. Hence, the inclusion devices will alter the structural response of the parent frame since the natural frequencies of the structure are modified, and the device will introduce hysteretic damping. Modelling of hysteretic behaviours is important especially in the field of structural engineering as it is impractical to obtain the performances of the dampers solely by experimental approach. It is costly and time consuming especially in optimizing the designs of the dampers. Therefore, this study not only applies the NARX model to predict the hysteretic response of the passive control systems but also demonstrate how to optimize the geometrical parameters of the passive control systems. The hysteretic behaviour of the passive dampers can be described by different mathematical models [10–14]. The analytical description of hysteretic response was first formulated by Bouc [15] and later generalized by Wen [10] as the generalized Bouc–Wen (BW) model. The generalized BW model proposed by Wen [10] was further extended to the Bouc–Wen–Baber–Noori (BWBN) hysteretic model [11–14] as the BW model does not include the properties of pinching and stiffness degradation. The BWBN is thus one of the famous models for simulating the hysteretic systems because it provides smooth hysteretic and also account for pinching and stiffness degradation.

This section introduced the passive energy dissipation systems and the importance of the modelling of hysteretic behaviour. The next section briefly describes the design of the yielding shear panel device (YSPD) employed for the model development in this study. Section 3 explains the reason of using artificial intelligence to predict the hysteretic behaviour of passive control systems. Section 4 introduces the design of the nonlinear-autogressive models with exogenous input (NARX) model, both of the architecture and algorithms of the NARX model will be covered. Section 5 reports the results of the hysteretic behaviour modelled by the NARX model. In Section 6, we combine the NARX model and general regression neural network (GRNN) as a hybrid model and use it to predict the steel slit damper (SSD) of which the damper design was hidden from the model training process. We also demonstrated the applicability of the hybrid model through the optimisation of the geometrical parameters of the SSD in Section 7. Finally, Section 8 provides a conclusion of this paper.

2. The design of yielding shear panel device (YPSD) and its test

The design of the YPSD is shown in Fig. 2. It is fabricated from a short segment of a square hollow section (SHS) with a steel diaphragm plate welded inside the SHS. The YSPD acts in shear as the parent frame structure undergoes lateral deformation. The input energy is dissipated through shear yielding of the diaphragm plate while the relative horizontal displacement between the top and bottom connections of the plate is sufficiently large.

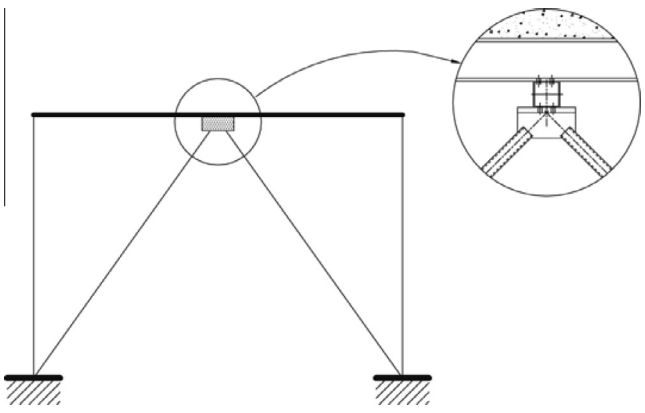

Fig. 1. Frame-brace-device assembly.

Table 1 summaries the details of the test specimens prepared for the test reported in [6]. There are two different SHS sections (i.e., $100 \times 100 \times 4$ and $120 \times 120 \times 5$), three diaphragm plate thicknesses (i.e., 2, 3 and 4 mm) were used and total 19 tests carried out on the YSPD were reported in [6]. The nomenclature used in the test is $D - tM$ or $D - tC/D - tCS$, where D indicates the size of the SHS section (i.e., 100 or 120 mm), t is the thickness of the diaphragm plate (i.e., 2, 3 or 4 mm). The letter M and C represent the monotonic test and cyclic test, respectively. The letter S represents a stiffened section.

Fig. 3 shows the experimental setup. The setup was designed and fabricated to ensure the verticality of the applied load. Forced displacement was applied by an MTS 100 kN capacity computer-controlled actuator quasi-statically to the specimen via the L-beam, where a pantograph system was attached to prevent its in-plane rotation. The test specimens were securely fastened by four M16 bolts on each side. The complete test setup rested on a 40-ton reaction frame which was significantly stiffer. A free-run of the setup indicated that effect of friction and gravity was negligible.

Experiment was carried out for each specimen to obtain the transmitted shear force through the damper under the specified forced displacement with 3 consecutive cycles performed at each amplitude (i.e., 0.5, 1.0, 3.0, 5.0, 10.0, and 20.0 mm). The time history of the forced displacement and the induced shear force across the dampers were recorded. Readers may refer to [6] for the details of the experiment.

3. The reason of using Nonlinear-Autoregressive-Exogenous (NARX) model to predict the hysteretic behaviour

Li et al. [16] successfully applied the BWBN model to simulate the hysteretic behaviour of the yielding shear panel device (YSPD) designed by [6]. The BW model owns the feature of versatility and mathematical tractability. It has widely applied to a variety of engineering problems. The generalized BW model and its extensions like the BWBN model have been used in the modelling and analysis of structural materials [13]. In Li et al. [16] study, Simulink was used to develop the BWBN model of the YSPD. The developed pinching model adopted in [16] provides a reasonable estimation of cumulative energy dissipation (i.e., within 10%). However, there were up to 16 parameters of the BWBN required to be calibrated to match with the experimental results. It requires a considerable length of time and computational resources to calibrate 16 parameters of the BWBN model. Therefore, this paper proposes an alternative approach to predict the hysteretic behaviours of the passive energy dissipation systems by the use of artificial intelligence with fewer components to be calibrated.

From an historical point of view, the moving average (MA), the autoregressive moving average (ARMA), and the linear parametric autoregressive (AR) models were the most common approaches for handling time-dependent problems before the 1980s [17]. Since the algorithms for MA and the parameters estimation models like AR are linear. They are not applicable for predicting non-linear time-series problems. At the same time, artificial neural networks (ANNs) drew a lot of people attention due to the characteristic of non-linear and non-parametric in nature. ANNs do not require assumptions about the problem under investigation, given that they are data-driven adaptive models and can learn the non-linear behaviour of a system from the historical data of the system. ANNs are suitable for problems whose solutions do not require prior knowledge of the system and they have been proven to be universal function approximators [18], current application of the ANNs

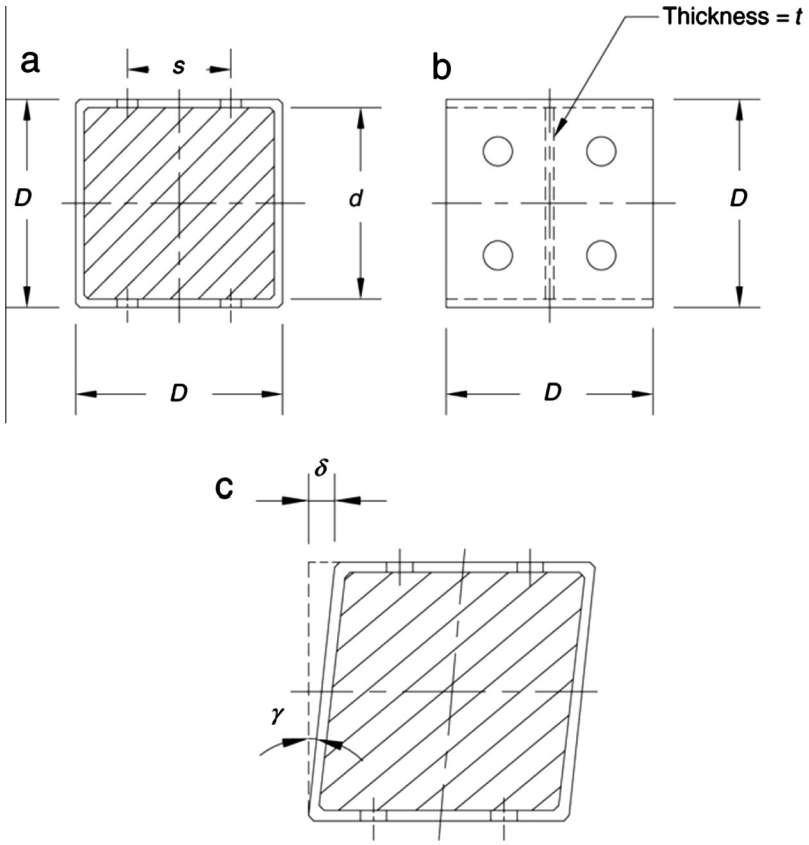

Fig. 2. Design of the YSPD (a) elevation, (b) top view and (c) deformed shape.

Table 1
Dimensions of the test specimens (unit: mm) of YSPD.

Test number	Specimen	SHS	Test regime
1	100-0 M	100 × 100 × 4	Monotonic
2	100-2 M		
3	100-3 M		
4	100-4 M		
5	100-0C	100 × 100 × 4	Cyclic
6	100-2C		
7	100-3C		
8	100-4C		
9	100-2CS		
10	100-3CS		
11	100-4CS		
12	120-0 M	120 × 120 × 5	Monotonic
13	120-2 M		
14	120-3 M		
15	120-4 M		
16	120-0C	120 × 120 × 5	Cyclic
17	120-2C		
18	120-3C		
19	120-4C		

can be found in [19–21]. There were few applications of NARX models for representation of hysteresis phenomena. Worden and Barthorpe [22] applied the NARX model for the identification of Bouc-Wen hysteretic systems. The data used for demonstration was generated by computer simulation. Leva and Piroddi [23] also applied NARX to model the magneto-rheological damping devices. In their study, computer generated data was used for evaluation of the model performance. In this study, experimental data obtained from [3,6] was used to evaluate the model performance.

4. The architecture of NARX model

Hysteretic systems have memory, the resisting force depends on both instantaneous deformation and past history of the deformation [14]. Therefore, the hysteretic behaviour of the passive control systems shall be suitable to be modelled by the NARX model. The NARX model is one of the artificial neural network models for time series prediction. It learns the behaviour of a system in a more effective way than other neural networks (i.e., the learning gradient algorithm is better in NARX) and also converges much faster and generalizes better than other networks [24]. Therefore, the NARX model is not only commonly applied in forecasting the time series cases but also important for the control of the dynamical systems. It has been demonstrated that they are capable to predict the behaviours of the nonlinear dynamics systems and particularly useful for time series modelling [25,26].

The structure of the NARX model is similar to the traditional multi-layered perceptron (MLP) model [27]. Among the various ANN models, the MLP model is one of the most widely used for forecasting due to its simple and flexible nature. Both MLP model and NARX model consist of an input layer, a hidden layer and an output layer but the NARX model feeds the time history of the output signal to the input layer as part of the inputs. The current input signal together with its time history acts as the other part of the inputs to the model. The number of output neurons equals to the number of output variables of the problem to be solved. The number of hidden neurons is required to be determined by the user. Assume Γ is the function of the NARX model. It correlates the input time series $\{u_t\}_{t=0}^{T}$ and the output time series $\{y_t\}_{t=0}^{T}$ by the Eq. (1).

$$y_t = \Gamma(y_{t-1}, y_{t-2}, \cdots, y_{t-\tau_y}, u_t, u_{t-1}, \cdots, u_{t-\tau_u}) \quad (1)$$

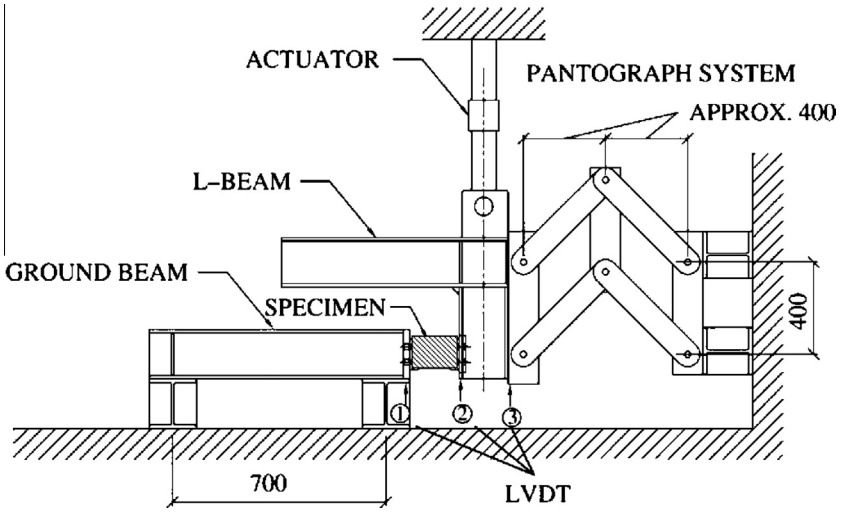

Fig. 3. Overview of the experimental setup.

where u_t and y_t represent the input and output of the network at time t, the function Γ is a nonlinear function, τ_y and τ_u are the time lags for the input and output series.

The general architecture of the NARX model is shown in Fig. 4. For this study, the output of the NARX model is the induced shear force across the dampers and the inputs of the NARX model is the time histories of the forced displacement and the induced shear force across the damper. Similar to the MLP model, each neuron has a bias input. The activation functions of the neurons in the input and output layers are linear while that of all hidden neurons is sigmoid function. Once the number of hidden neurons is determined, the total number of the weighting factors between each neuron can also be found. For the learning process, the Levenberg–Marquardt algorithm is adopted in this study due to the fast convergence properties. The performance index used in NARX model training is the mean squared error (MSE), which is one of the typical performance functions as shown in Eq. (2).

$$MSE = \frac{1}{N_s}\sum_{i=1}^{N_s}(t_i - y_i)^2 \tag{2}$$

where t_i and y_i represent the target and the output of the network and N_s is the number of training samples.

5. Prediction of YSPD by the NARX model

Section 2 detailed the design of the YSPD reported in [6], Section 3 and 4 explained the reason of using the NARX model to predict the hysteretic behaviour and the general architecture of the NARX model, respectively. This section presents the results which predicted by the NARX model. The experimental hysteretic responses of YSPD were reported in [6]. For comparing the results predicted by NARX with Li et al. [16], six of the specimens (i.e., 100-2C, 100-2CS, 100-3C, 100-3CS, 120-2C and 120-3C) were used in the current study to evaluate the performance of the trained NARX model. After several trials, it was found that the optimal setting of the required time lags for the input and output series is 2 (i.e., $\tau_y = \tau_u = 2$). The architecture of the NARX model adopted in this study to predict the hysteretic response of the YSPD is shown in Fig. 5. Only one hidden neuron is used to develop the NARX model throughout this study, in which the number of weighting factors to be calibrated for the prediction of hysteretic responses is 8 (i.e., w_1 to w_8).

The comparison of the experimental hysteretic responses in the cyclic tests of six YSPD and the prediction results by using the NARX model are shown in Fig. 6. The crosses in Fig. 6 represent

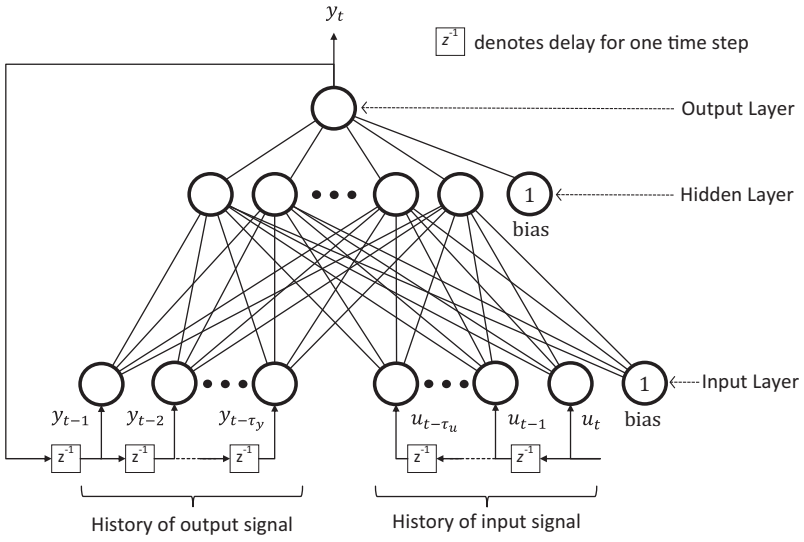

Fig. 4. General architecture of the NARX model.

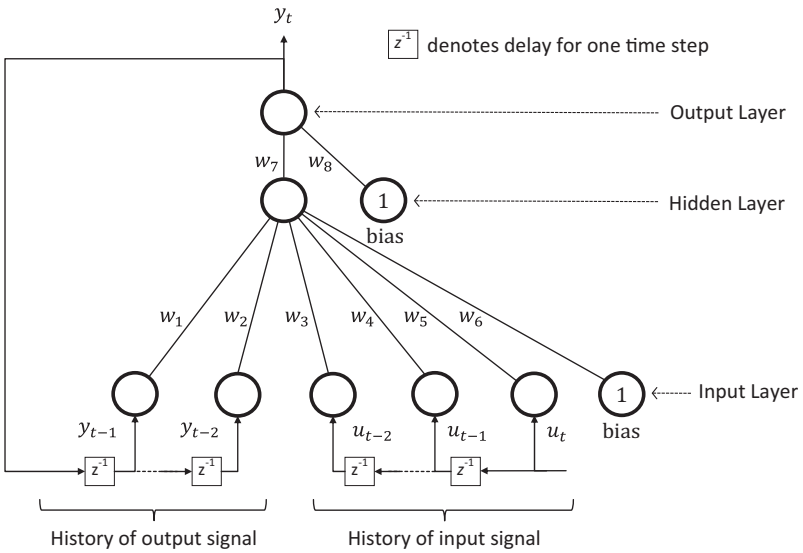

Fig. 5. Architecture of the NARX model adopted in this study.

the target value which obtained from the experimental study in [6], while the solid lines represent the predicted output which estimated by the NARX model proposed in this study. The positive direction refers to downward induced shear force and displacement in the force–displacement hysteresis.

The predicted results of the NARX model show a good agreement with the experimental results. Both of the predicted result and experimental result of Specimen 100-2C exhibit reasonably stable hysteretic with a slightly pinched hysteretic near zero displacement in the last cycle (i.e., caused by shear buckling). Similar hysteretic behaviour can also be observed for the stiffened specimen 100-2CS. Specimens with thicker diaphragm plates (100-3C and 100-3CS) did not show buckling, but exhibit a more pronounced pinched hysteretic loops near the zero displacement due to localized deformation near the bolt connections. Specimen 120-2C and 120-3C performed satisfactorily with state and large force displacement hysteretic.

Li et al. [16] used Simulink to develop the BW and BWBN models to predict the hysteretic responses of YSPD. There were up to 16 parameters of the BWBN required to be tuned to match with the experimental results. In this study, we demonstrated how to use the NARX model with only one hidden neuron to predict the hysteretic behaviour. Table 2 compares the amount of cumulative energy dissipation predicted by using the BW and BWBN models developed in [16], the experimental results and the NARX models. The area of the hysteresis loops represents the cumulative energy dissipation by the passive energy dissipation systems. The results obtained by Li et al. [16] provide a good estimation of the cumulative energy dissipation, the absolute percentage error of the cumulative energy dissipation between the experimental results and the results predicted by the BWBN models is ranged from 0.57% to 9.77% which is superior to the result predicted by the BW models (i.e., ranged from 2.43% to 52.86%) as the pinching behaviour was also considered in the BWBN models. On the other hand, the trained NARX models with one hidden neurons provide a very promising estimation of the cumulative energy dissipation, the absolute percentage error of the cumulative energy dissipation between the experimental results and the results predicted by the NARX models is ranged from 0.00599% to 0.75% for all specimens. It shows a better performance than both BW and BWBN models with only total 8 numbers of weighting factors to be calibrated. The poor performance of BW and BWBN models may be caused by the over-simplification of the hysteretic behaviour in the differentiation equations of the BW and BWBN models.

6. Prediction of SSD by the hybrid model

Section 5 presented the prediction of the hysteretic behaviour of the YSPD by the NARX model. The prediction results depicted the applicability of the NARX model in hysteretic behaviour prediction of passive control systems. In this section, we combine the NARX model and the GRNN model as a hybrid model to predict the mechanical response of a new damper design of which the geometrical parameters of the damper was hidden from the NARX model training. In this study, we adopted the experimental results of SSD from [3] to benchmark the performance of the hybrid model. The design of the experiment of the SSD is introduces as follows.

Fig. 7 shows the design of the Steel Slit Damper. It is fabricated from a standard structural I-section with a number of slits introduced the web, forming a vierendeel truss arrangement. The strips are filleted to reduce stress concentrations. Each flange is connected to the main structure by four structural bolts. It is a weld-free design, eliminating heat-affected imperfections associated with welding.

Table 3 summaries the dimensions of the six specimens (i.e., SL-01 to SL-06) presented in this study. To eliminate variability in material properties, all specimens were cut from the same structural I-section ($152 \times 152 \times 37$ Universal Column to BS4449). Strip thickness t and material strengths of all specimens were assumed equal. Four 16 mm diameter holes were drilled on each flange. Two standard test coupons were taken from the web of the section. An average tensile yield stress of 316.5 N/mm^2 and an average Modulus of Elasticity of 206.1 kN/mm^2 were obtained by standard tensile tests. Each specimen weighed approximately 2.2 kg. Readers may refer to [3] for the details of the experiment.

Fig. 8 shows the domain of the geometrical parameters of the SSD reported in [3]. It can be observed that specimen SL-02 is laid slightly outside the boundary of the domain. In general, the ANN models are developed from the historical data of a system. The ANNs can perform very well for the prediction inside the domain of a system, but not outside the domain of the system. Therefore, we propose to use the hybrid model to predict the hysteretic

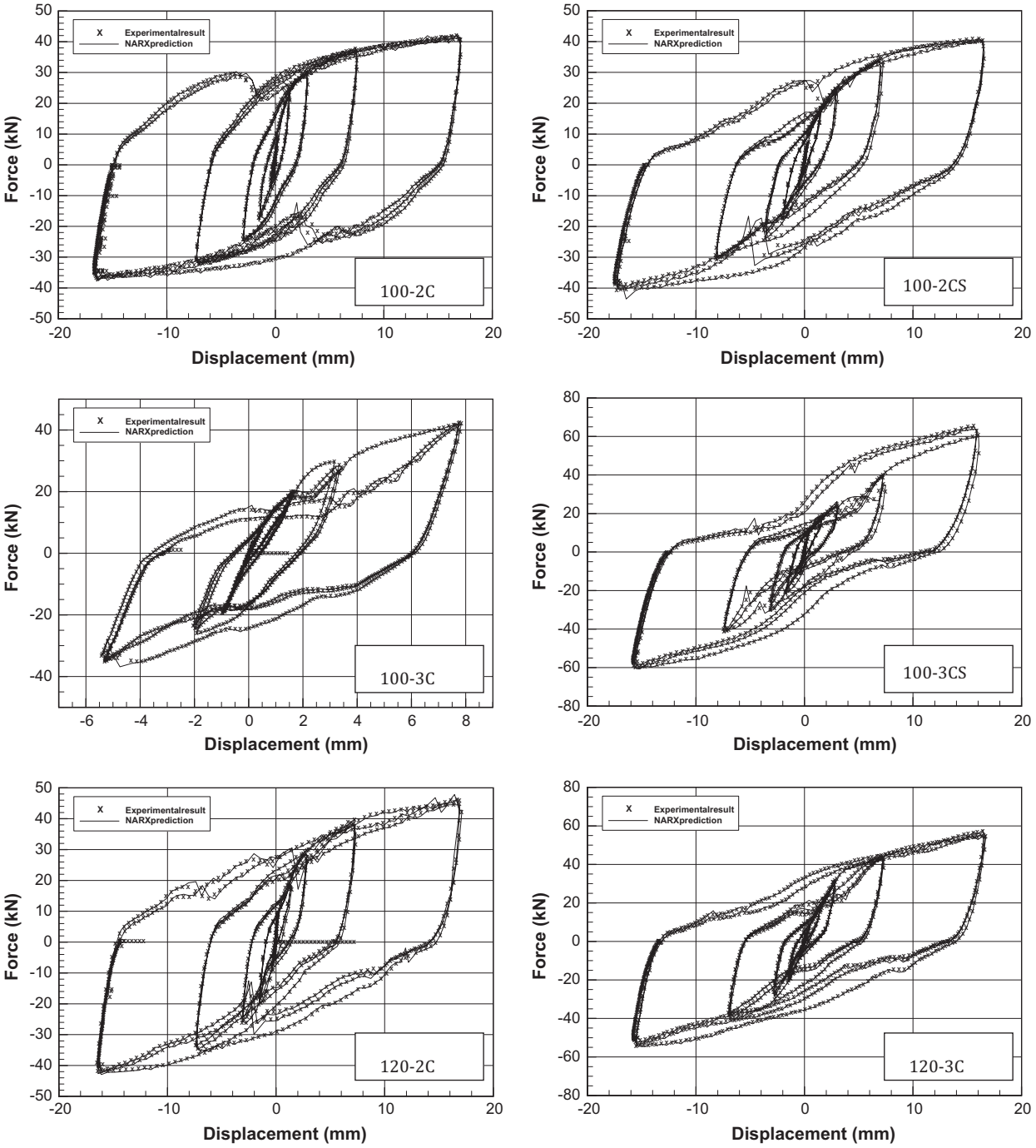

Fig. 6. Hysteretic behaviours of the specimens (100-2C to 120-3C) of YSPD predicted by the NARX model.

Table 2
Comparison of hysteretic energy dissipation of YSPD from different models.

Specimen	Experimental results	Energy dissipation in kJ, (absolute percentage error)		
		BW model	BWBN model	NARX with one hidden neuron
100-2C	6.99	7.16 (2.43%)	6.95 (0.57%)	6.98 (0.14%)
100-3C	1.33	1.92 (44.36%)	1.46 (9.77%)	1.32 (0.75%)
100-2CS	5.73	6.92 (20.77%)	5.79 (1.05%)	5.73 (0.00599%)
100-3CS	5.94	9.08 (52.86%)	6.39 (7.58%)	5.93 (0.17%)
120-2C	6.23	7.28 (16.85%)	6.45 (3.53%)	6.21 (0.32%)
120-3C	6.51	7.65 (17.51%)	7.10 (9.06%)	6.49 (0.31%)

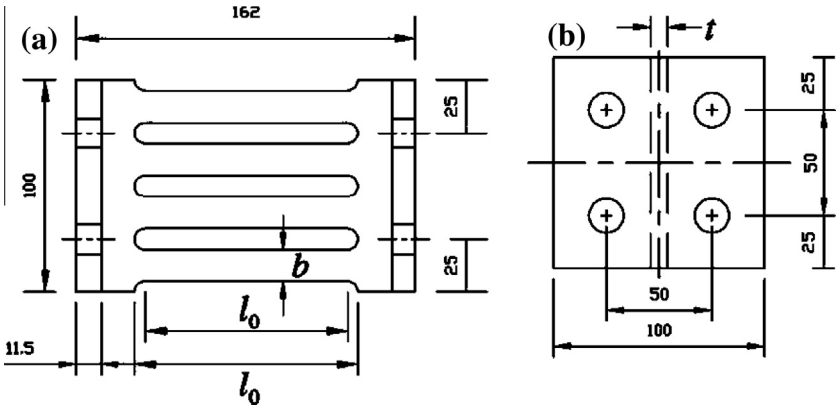

Fig. 7. Design of the SSD (a) elevation and (b) top view.

Table 3
Dimensions of the test specimens (unit: mm) of SSD.

Specimen ID	Measured dimensions			b/l_0
	Web thickness, t	Strip depth, b	Strip length, l_0	
SL-1	8.0	14.9	97.0	0.155
SL-2	8.0	15.0	87.1	0.172
SL-3	8.0	15.1	77.0	0.195
SL-4	8.0	16.9	99.2	0.172
SL-5	8.0	16.8	88.3	0.191
SL-6	8.0	16.5	79.0	0.215

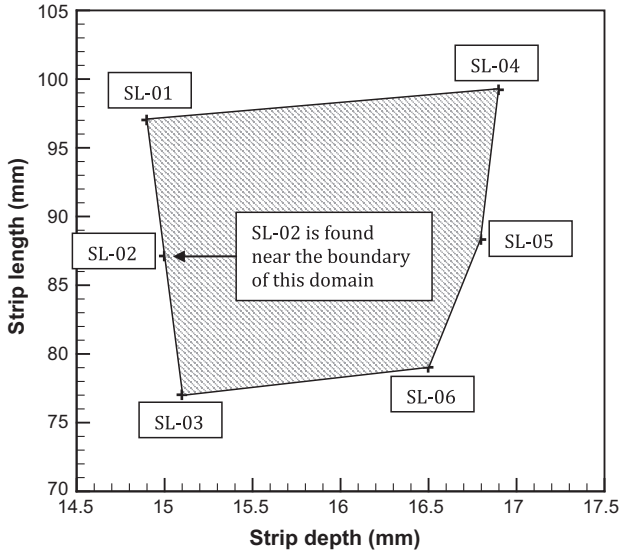

Fig. 8. Domain of the geometrical parameters of the SSD.

behaviour of specimen SL-02 from the experimental data of specimens SL-01, SL-03 to SL-06 as the hysteretic behaviour of specimen SL-02 is the nearest specimen to the boundary of the domain.

The hybrid model proposed in this study for predicting the hysteretic behaviour of the SSD is a combination of the NARX model and the GRNN model. The GRNN was presented by Specht in 1991 [28], which is a memory-based network. It provides estimate of continuous variable and converges to the underlying regression surface even with sparse sample. The GRNN recruits every training sample as a kernel in its model, and thus users do not need to predefine the network structure. It has been successfully applied to a variety of fields such as image processing, non-linear adaptive control and machinery fault diagnosis owing to the simple network structure, fast network training time, powerful regression properties, and ease of implementation [29–31].

The GRNN model, in fact, computes the expected conditional mean of a probability distribution in condition with the given input vector. The key step of the GRNN model is to establish the probability distribution density of the joint input and output spaces according to the information of the training samples. Parzen density estimator [32] is employed for the density establishment. Assume $\boldsymbol{X} = \{x_1, x_2, \cdots, x_n\} \in \Re$ are samples taken from a one dimensional domain with underlying probability density function $\hat{Y}(X)$, the fundamental formulation of the GRNN is deduced as follows.

$$\hat{Y}(\boldsymbol{X}) = \frac{\sum_{i=1}^{N_s} Y^i e^{(-D_i^2/2\sigma^2)}}{\sum_{i=1}^{N_s} e^{(-D_i^2/2\sigma^2)}} \tag{3}$$

$$D_i^2 = (\boldsymbol{X} - \boldsymbol{X}^i)^{\mathrm{T}} (\boldsymbol{X} - \boldsymbol{X}^i) \tag{4}$$

where $\hat{Y}(\boldsymbol{X})$ is the desired conditional mean associated with the input $\boldsymbol{X}$, σ is the smoothness parameter (i.e., the kernel width of the Gaussian function), N_s is the number of training samples, and D_i is the Euclidean distance between the training sample, X and the point of prediction X^i. Different from the traditional MLP or NARX model, once the input of GRNN is given, GRNN is capable to determine the architecture and weights by itself. Therefore, training GRNN is essentially to optimize the smoothness parameter only, to obtain the optimal regression prediction.

The GRNN model is proposed to combine with the NARX model as a hybrid model to predict the hysteretic response of SSD of which the damper design was hidden from the NARX model training. The network structure of the hybrid model is similar to the GRNN model. From Eqs. (3) and (4), the hybrid model is constructed as shown in Fig. 9. It is with multi inputs and one single output, and consists of 4 layers of neurons, namely input, pattern, summation and output layer.

In this study, the number of the input units in input layer is 2. These 2 neurons represent the geometrical parameters (i.e., strip length, l_0 and the strip depth, d) of the specimen SL-02, respectively. The input layer is connected to the pattern layer and in this layer each neuron presents a training pattern and its output. There are total 5 numbers of neurons in the pattern layer (i.e., specimen SL-01, SL-03 to SL-06 and specimen SL-02 was hidden during the model training process). They calculate the Euclidean distance of the training sample from the neuron's center and apply the Gaussian function with the predefined smoothness parameters (i.e., $e^{(-D_i^2/2\sigma^2)}$). The resulting value is then passed to the neurons in the summation layer. In the summation layer, the numerator summarizes the products of weight values and the resulting values

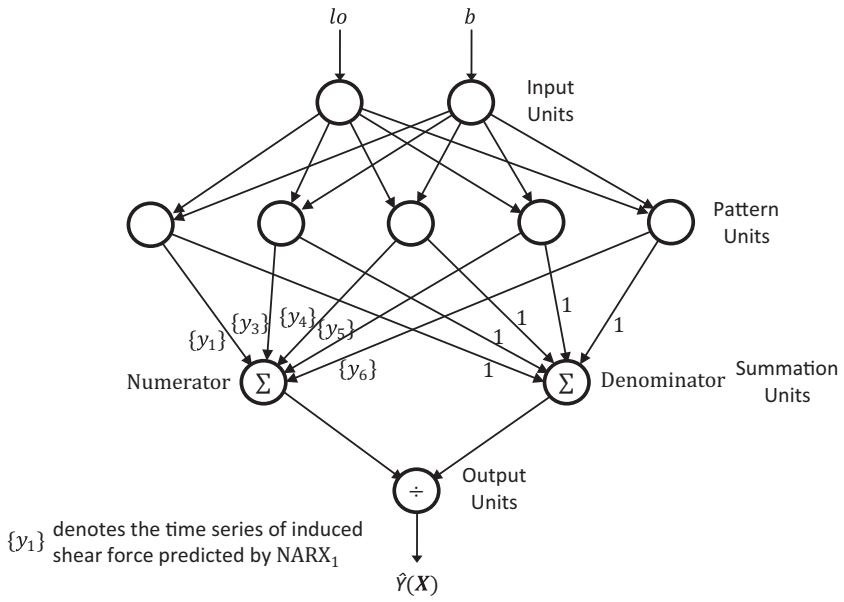

Fig. 9. Architecture of the hybrid model (GRNN model with NARX model).

obtained from the pattern layer. In which, the weights ($\{y_1\}$, $\{y_3\}$ to $\{y_6\}$) between the pattern layer and the numerator are the time series obtained by the NARX models presented in Section 5. For example, the time series $\{y_1\}$ is obtained by the NARX model which developed from the time histories of the displacement and the induced shear force of specimen SL-01 reported in [3]. The denominator also summarizes the products of weight values and the resulting values obtained from the pattern layer. But in this case, the weights on the signals going into the denominator neuron are one. Finally, the output layer divides the accumulated value in the numerator by the value in the denominator and the time series of the induced shear force of specimen SL-02 can be obtained.

After several trials, the smoothness parameter (σ) was determined to be 50. Fig. 10 shows the hysteretic behaviours of the dampers predicted by the NARX model and GRNN. Table 4 compares the amount of cumulative energy dissipation predicted by using the hybrid model and the experimental results. The amount of cumulative energy dissipation predicted by using NARX models and the hybrid are also presented to benchmark the performance of the hybrid model. The trained NARX models with only one hidden neuron provide very a promising estimation of the cumulative energy dissipation, the absolute percentage error of the cumulative energy dissipation between the experimental results and the results predicted by the NARX models is ranged from 0.0662% to 0.30% for all the specimens of the SSD. The performance of using the hybrid model to predict the hysteretic behaviour of SSD is reasonably well. The absolute percentage error of the cumulative energy dissipation between the experimental results and the results predicted by the hybrid models of specimen SL-02 is 6.97%. It concluded that the application of the hybrid model is capable to predict the hysteretic behaviour of a new design of passive control systems.

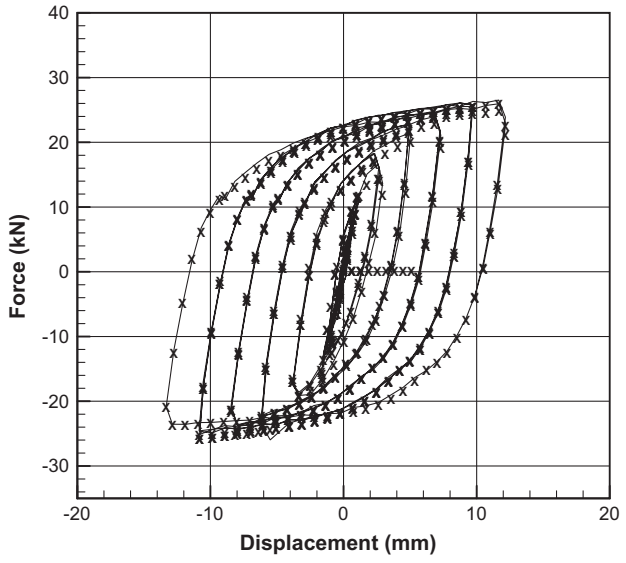

Fig. 10. Hysteretic behaviours of the SSD (SL-02) predicted by the hybrid model.

7. Application of the hybrid model to optimize the geometry of the SSD

This section demonstrates the application of the developed hybrid model with GAs [33] for passive control system design. The advantage of GAs over conventional searching algorithms is that GAs can deal with a wide range of areas and are able to find 'acceptable' solutions in a reasonable time. They have also been shown to be superior to conventional optimisation techniques, especially for discontinuous and noisy functions [34].

The passive control system is designed for minimizing the damage of the structures caused by earthquake excitation, the larger the energy dissipated by the damper, the better the performance of the passive control system is. To mitigate the energy generated during the earthquake, the designer is required to determine the geometrical parameters of the passive control damper properly. Therefore, it is important to maximize the damper's effectiveness at minimum cost [35]. We propose to use the developed hybrid model with GAs to optimize the geometrical parameters of the SSD reported in [3], such that the energy dissipation can be maximized. Eq. (5) is the fitness function to be minimised in the GAs optimisation to achieve this design objective, where $\int_a^b f(x)dx$ is

Table 4
Comparison of hysteretic energy dissipation of SSD from different models.

Specimen	Experimental results	Energy dissipation in kJ, (absolute percentage error)	
		NARX with one hidden neuron	Hybrid model (NARX with GRNN models)
SL-01	8.17	8.18 (0.12%)	–
SL-02	6.60	6.62 (0.30%)	7.06 (6.97%)
SL-03	5.95	5.96 (0.17%)	–
SL-04	8.92	8.92 (0.0662%)	–
SL-05	6.79	6.79 (0.0781%)	–
SL-06	7.38	7.40 (0.27%)	–

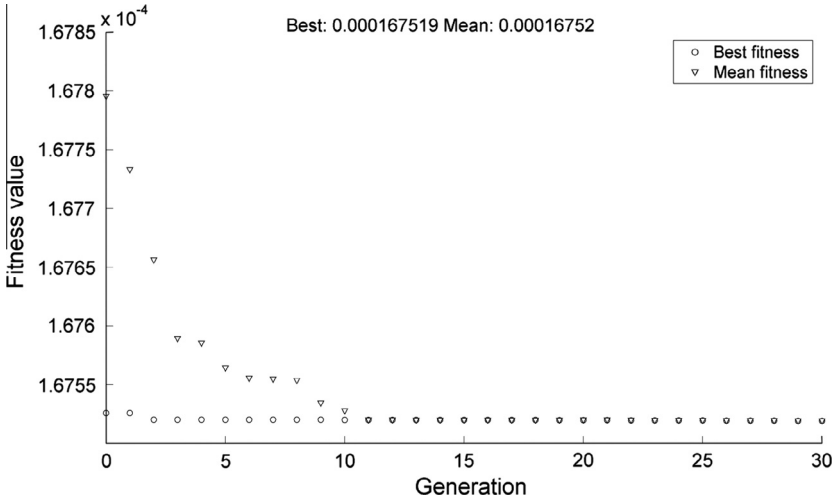

Fig. 11. Fitness value versus generation during the optimisation process.

the energy dissipation of the damper and it can be approximated by using the numerical method like trapezoidal rule as shown in Eq. (6) in which f and x represent the induced shear force across the damper and the displacement of the damper, respectively. Therefore, the result is converged if the fitness value reaches the minimum.

$$fitness\ value = \frac{1}{\int_a^b f(x)dx} \tag{5}$$

$$\int_a^b f(x)dx \approx \frac{\sum_{i=1}^{\frac{b-a}{\Delta x}}(f_{i+1}-f_i)}{2} \tag{6}$$

As explained in Section 6, ANN models are developed from the historical data of a system. They perform well for the prediction inside the domain of a system. Therefore, some constraints are listed as follow to provide a bounded condition for the optimization:

1. Lower Boundary is added to ensure the minimum strip depth and length is within the boundary of the domain as reported in [3] (i.e., b $\geqq$ 14.9 mm and $l_0 \geqq$ 77.0 mm).
2. Upper Boundary is added to ensure the maximum strip depth and length is within the boundary of the domain as reported in [3] (i.e., $b \leqq$ 16.9 mm and $l_0 \leqq$ 99.2 mm).

The optimization process involve both of the hybrid model and GA model. The main purpose of the hybrid model is to estimate the cumulative energy dissipation of the SSD and the GA model is to search the optimum strip depth and length to minimize the fitness function as shown in Eq. (5). During the optimization process, the fitness value is converged at approximately 12 generation and the best fitness value is 1.6719×10^{-4} (i.e., the cumulative energy dissipation is 5969.47 kJ. The optimised strip depth and length are 16.8853 and 77.0002, respectively. The process of optimization is shown in Fig. 11.

8. Conclusion

In this paper, the hysteretic behaviour of the passive control systems in structures is proposed to be modelled by the NARX model. The performance of the prediction is evaluated and the prediction results show a good agreement between the experimental results and the predicted outputs for both YSPD and SSD. The maximum absolute percentage error of the cumulative energy dissipation between the experimental results and the results predicted by the NARX models of the YSPD and SSD are 0.75% and 0.30%, respectively. It indicates a reliable prediction to the experimental results by using the NARX model. We also presented the hybrid model which is the combination of the NARX model and GRNN model to predict the hysteretic behaviour of SSD of which the damper design was hidden from the NARX model training. The hysteretic behaviour of the SSD can also be successfully modelled by the hybrid model. The absolute percentage error of the cumulative energy dissipation between the experimental results and the result predicted by the hybrid model is 6.97%, which is a reasonably good prediction. Finally, the applicability of the hybrid model has been successfully demonstrated through the optimisation of the geometrical parameters of the SSD.

Acknowledgement

The work described in this paper was fully supported by a grant from the Research Grant Council of the Hong Kong Special Administrative Region [Project No. CityU 116613].

References

[1] Soong TT, Dargush GF. Passive energy dissipation systems in structural engineering. John Wiley & Sons; 1997.
[2] Soong TT, Spencer Jr BF. Supplemental energy dissipation: state-of-the-art and state-of-the-practice. Eng Struct 2002;24:243–59.
[3] Chan RWK, Albermani F. Experimental study of steel slit damper for passive energy dissipation. Eng Struct 2008;30(4):1058–66.
[4] Bergman DM, Goel SC. Evolution of cyclic testing of steel plate devices for added damping and stiffiness. Report No. UMCE87-10. Ann Arbor: The University of Michigan; 1987.
[5] Tena-Colunga A. Mathematicla modelling of the ADAS energy dissipation device. Eng Struct 1997;19(10):811–21.
[6] Chan RWK, Albermani F, Williams MS. Evaluation of yielding shear panel device for passive energy dissipation. Construct Steel Res 2009;65(2):260–8.
[7] Benavent-Climent A. A brace-type seismic damper based on yielding the walls of hollow structural sections. Eng Struct 2010;32(4):1113–32.
[8] Briones B, De la Llera JC. Analysis, design and testing of an hourglass-shaped copper energy dissipation device. Eng Struct 2014;79:309–21.
[9] Koetaka Y, Chusilp P, Zhang Z, Ando M, Suita K, Inoue K, et al. Mechanical property of beam-to-column moment connection with hysteretic dampers for column weak axis. Eng Struct 2005;27:109–17.
[10] Wen YK. Method for random vibration of hysteretic systems. J Eng Mech Div, ASCE 1976;102:249–63.
[11] Baber TT, Wen YK. Random vibration of hysteretic degrading systems. J Eng Mech, ASCE 1981;107:1069–89.
[12] Baber TT, Noori MN. Modeling general hysteretic behaviour and random vibration application. J Vibr Acoust Stress Reliab Design-Trans, ASME 1986;108:411–20.
[13] Foliente GC, Singh MP, Noori MN. Equivalent linearization of generally pinching hysteretic, degrading systems. Earthq Eng Struct Dyn 1996;25:611–29.
[14] Mostaghel N. Analytical description of pinching degrading hysteretic systems. J Eng Mech 1999;125(2):216–24.
[15] Bouc R. Modele Mathematique D'Hysteresis. Acustica 1967;24(1):16–25 [in French].
[16] Li Z, Albermani F, Chan RWK, Kitipornchai S. Pinching hysteretic response of yielding shear panel device. Eng Struct 2011;33:993–1000.
[17] Pollok DSG. A handbook of time-series, signal processing and dynamics. Academic Press; 1999.
[18] Hornik K, Stinchcombe M, White H. Multilayer feed forward networks are universal approximators. Neural Networks 1989;2:359–66.
[19] Yuen JKK, Lee EWM, Lo SM, Yuen RKK. An intelligence-based optimization model of passenger flow in a transportation station. IEEE Trans Intell Transp Syst 2013;14(3):1290–300.
[20] Yuen RKK, Lee EWM, Lo SM, Yeoh GH. Prediction of temperature and velocity profiles in a single compartment fire by an improved neural network analysis. Fire Saf J 2006;41(6):478–85.
[21] Li DHW, Tang HL, Lee EWM, Muneer T. Classification of CIE standard skies using probabilistic neural networks. Int J Climatol 2010;30(2):305–15.
[22] Worden K, Barthorpe RJ. Identification of hysteretic systems using NARX Models, Part I: evolutionary identification. Conference Proceedings of the Society for Experimental Mechanics Series 2012;4:49–56.
[23] Leva A, Piroddi L. NARX-based technique for the modelling of magneto-rheological damping devices. Smart Mater Struct 2002;11:79–88.
[24] Lin T, Horne BG, Tino P, Giles CL. Learning long-term dependencies in NARX recurrent neural networks. IEEE Trans Neural Netw 1996;47(6):1329–51.
[25] Chen S, Bilings SA, Grant PM. Non-linear system identification using neural networks. Int J Control 1990;51(6):1191–214.
[26] Leontaritis IJ, Bilings SA. Input-output parametric models for non-linear systems: Part IL deterministic non-linear systems. Int J Control 1985;41(2):303–28.
[27] Rosenblatt F. Principles of neurodynamics. New York: Spartan Books; 1962.
[28] Specht DF. A general regression neural network. IEEE Trans Neural Networks 1991;2(6):568–76.
[29] Rzempoluck EJ. Neural network classification of EEG during camouflaged object identification. Int J Med Inform 1997;44:169–75.
[30] Schaffner C, Schroder D. An application of general regression neural network to nonlinear adaptive control. EPE 1993;4:219–24.
[31] Hyun BG, Nam K. Faults diagnoses of rotating machines by using neural nets: GRNN and BPN. In: Proceedings of the 1995 IEEE IECON 21st international conference on industrial electronics, control, and instrumentation 1995, vol. 2. p. 1456–61.
[32] Parzen E. On estimation of a probability density function and mode. Ann Math Stat 1962;33:1065–76.
[33] Holland JH. Adaptation in natural and artificial systems. MIT Press; 1975.
[34] Beasley D, Bull DR, Martin RR. An overview of genetic algorithms: Part 1, Fundamentals. University Computing 1993;41(2):58–69.
[35] Wu B, Ou JP, Soong TT. Optimal placement of energy dissipation devices for three-dimensional structures. Eng Struct 1997;19(2):113–25.